A Regulatory Path Associated with X-Linked Intellectual Disability and Epilepsy Links *KDM5C* to the Polyalanine Expansions in ARX

Loredana Poeta,[1,2] Francesca Fusco,[1] Denise Drongitis,[1] Cheryl Shoubridge,[3,4] Genesia Manganelli,[1,5] Stefania Filosa,[1,5] Mariateresa Paciolla,[1,2] Monica Courtney,[6,7] Patrick Collombat,[6,7] Maria Brigida Lioi,[2] Jozef Gecz,[3,4] Matilde Valeria Ursini,[1] and Maria Giuseppina Miano[1,*]

Intellectual disability (ID) and epilepsy often occur together and have a dramatic impact on the development and quality of life of the affected children. Polyalanine (polyA)-expansion-encoding mutations of aristaless-related homeobox (*ARX*) cause a spectrum of X-linked ID (XLID) diseases and chronic epilepsy, including infantile spasms. We show that lysine-specific demethylase 5C (*KDM5C*), a gene known to be mutated in XLID-affected children and involved in chromatin remodeling, is directly regulated by ARX through the binding in a conserved noncoding element. We have studied altered ARX carrying various polyA elongations in individuals with XLID and/or epilepsy. The changes in polyA repeats cause hypomorphic ARX alterations, which exhibit a decreased *trans*-activity and reduced, but not abolished, binding to the *KDM5C* regulatory region. The altered functioning of the mutants tested is likely to correlate with the severity of XLID and/or epilepsy. By quantitative RT-PCR, we observed a dramatic *Kdm5c* mRNA downregulation in murine *Arx*-knockout embryonic and neural stem cells. Such *Kdm5c* mRNA diminution led to a severe decrease in the KDM5C content during in vitro neuronal differentiation, which inversely correlated with an increase in H3K4me3 signal. We established that ARX polyA alterations damage the regulation of *KDM5C* expression, and we propose a potential ARX-dependent path acting via chromatin remodeling.

The most common causes of X-linked intellectual disability (XLID [MIM 300419]), after *FMR1* (MIM 309550) mutations, are polyalanine (polyA)-tract-expansion-encoding mutations in aristaless-related homeobox (*ARX* [MIM 300382]).[1,2] Additionally, ARX polyA-tract-expansion alterations have frequently been found to be associated with either frequent tonic seizures or spasms (West syndrome or epileptic encephalopathy early infantile 1 [EIEE1 (MIM 308350)])[1–4] or with dystonic movements, ataxia, and seizures (Partington syndrome [MIM 309510])[1,2,5] in children with pediatric epilepsy. The majority of ARX polyA individuals with pediatric seizures are resistant to traditional antiepileptic drugs; their cognitive development is thus affected, causing ID with different degrees of severity.[1,2] These particular epileptic phenotypes have been primarily associated with a deficit in the forebrain cerebrocortical-interneuron function, and this condition has thus been designated as an "interneuronopathy."[6] A striking and selective gamma-aminobutyric acid (GABA)ergic interneuronopathy was observed in the neocortex of *Arx*-knockin polyA disease models.[7,8] Located at Xp22.13, *ARX* is a homeobox gene encoding a paired-type-homeodomain (paired-HD) transcription factor (TF) of crucial significance for brain ontogenesis.[1] It has been implicated in numerous human congenital brain disorders.[1,9–15] In humans, in-frame duplications affecting polyA I and polyA II, two out of the four polyA amino acid tracts (polyA I, polyA II, polyA III, and polyA IV), represent disease hot spots and have a strong tendency to add coding trinucleotide repeats $(GCN)_n$.[2,16,17] These result in polyA-tract-expansion alterations, frequently present in male children with XLID alone,[15,18–21] XLID associated with seizures (XLID with epilepsy),[2,9,10] or XLID associated with dysarthria and dystonia (West syndrome or Partington syndrome).[3,5,22–26] In affected families, these duplications are stable during intergenerational transmission and display a rare postmitotic instability.[27] Hitherto, no alterations have been reported in polyA III or polyA IV. Despite the fact that the pathogenetic mechanisms have recently been revealed for some *ARX* missense mutations,[28] contradictory results have been obtained on the pathogenic consequences of ARX polyA alterations in cellular[21,29,30] and animal[7,8,31] model systems. To date, the functional disturbance of these particular *ARX* alleles on human target genes has not been established. In this study, we address this issue through the discovery that elongations in the polyA tracts of ARX perturb the expression of lysine-specific demethylase 5C (*KDM5C/JARID1C/SMCX* [MIM 314690]).[32,33] Located at Xp11.22, *KDM5C* encodes a histone demethylase specific to dimethylated and trimethylated histone 3 lysine 4 (H3K4me2 and H3K4me3, respectively), which are involved in chromatin remodeling.[34] Notably, mutations in *KDM5C* are emerging as a frequent cause of

[1]Institute of Genetics and Biophysics "Adriano Buzzati Traverso," Consiglio Nazionale delle Ricerche, Naples 80131, Italy; [2]University of Basilicata, Potenza 85100, Italy; [3]Department of Paediatrics, University of Adelaide, Adelaide, South Australia 5006, Australia; [4]Department of Genetics and Molecular Pathology, Adelaide, South Australia 5006, Australia; [5]Istituto Di Ricovero e Cura a Carattere Scientifico, Neuromed, Pozzilli 86077, Italy; [6]Université Nice Sophia Antipolis, Nice 06108, France; [7]Institut National de la Santé et de la Recherche Médicale Unité 1091, Diabetes Genetics Team, Institute of Biology Valrose, Nice 06108, France
*Correspondence: miano@igb.cnr.it
http://dx.doi.org/10.1016/j.ajhg.2012.11.008.

XLID (MIM 300534),[32,33] whose disease outcomes share overlapping epileptic symptoms with those of the ARX polyA alterations.[32–34]

By in silico search, we first verified the presence of the ARX binding motif 5′-TAATTA-3′[35] and/or a similar sequence[36] in the 5′ and 3′ conserved noncoding elements (CNEs) of human *KDM5C*. We thereby identified three putative ARX-binding sites (BD1, BD2, and BD3) in a stretch of 1,124 bp, termed CNE-5′JD, with a high nucleotide conservation (>75%) across four closely related mammals: *H. sapiens*, *C. familiaris*, *M. musculus*, and *B. taurus* (Figure S1, available online). CNE-5′JD is located 6.44 Kb downstream of IQ-motif- and sec7-domain-containing 2 (*IQSEC2* [MIM 300522]), recently found to be mutated in families affected by XLID (MIM 309530).[37] Both *KDM5C* and *IQSEC2* are head to tail with the first exon of *KDM5C* and are located 7.45 Kb downstream of the last exon of *IQSEC2*. The CNE-5′JD sequence was compared to TF-binding sites in TRANSFAC libraries. Because human ARX and its murine counterpart might have subtle differences in binding preference and strength,[36] we chose for further analysis the 10 nt palindromic DNA sequence composed of an inverted 5′-TAAT-3′ motif separated by two nucleotides 5′-TAAT$(N)_2$ATTA-3′ (BD1); the 4 nt single-module 5′-ATTA-3′ (BD2); and the 4 nt single-module 5′-TAAT-3′ (BD3). The sequences of the predicted binding sites are highly conserved and extremely similar to the 5′-TAATTA-3′ motif recognized in mice on the promoters of ARX-regulated genes[35,36] (Figures S1 and S2) and to the consensus sequences recognized by paired-HD TFs.[38]

We then sought to verify whether ARX transcriptionally activates *KDM5C*. A luciferase reporter construct with the CNE-5′JD region of *KDM5C* (−1,001/+73, pJD-full-Luc) was transiently transfected into four different mammalian cellular contexts (HeLa, SH-SY5Y, PC12, and P19 cells). We thus confirmed that the CNE-5′JD construct has real transcriptional activity (Figure 1A) and that in cotransfection with the pCMV expressing the wild-type (WT) ARX, its activity increased significantly in all cell lines: 84% in HeLa cells, 42% in SH-SY5Y cells, 80% in PC12 cells, and 31% in P19 cells (Figure 1A). Next, we examined the transcriptional relevance of each individual putative binding site. Luciferase analyses of the deleted constructs (Figure 1B) carrying both BD1 and BD2 (pJD/BD1-2) or just a single module (pJD/BD1 or pJD/BD2) (Figure 1B) in cotransfection with WT ARX revealed that each of them is required for the ARX-mediated activation of pJD-full-Luc. In addition, BD1 and BD2 could act cooperatively. Indeed, the transcriptional activity driven by pJD/BD1-2, carrying both the BD1 and BD2 sites, was higher than that in the constructs carrying the individual BD1 or BD2 site. It is noteworthy that pJD/BD3 and pJD/BD2-3 (data not shown) were not activated, suggesting the presence of a negative regulatory region located within the proximal region −401/+73 bp (Figure 1B). We also explored the specific role of each site by studying site-mutated (SI) constructs carrying selective point mutations of one (pJD/BD1_1°mut, pJD/BD1_2°mut, pJD/BD2mut, or pJD/BD3mut) or two modules (pJD/BD1mut) at a time (Figure 1C). We observed that mutations at the potential ARX-binding sites nullify the responsiveness of the CNE-5′JD element both in basal and ARX-activated conditions, suggesting that all three binding sites, BD1, BD2, and BD3, are required for *KDM5C* transcriptional activity. More interestingly, mutations in each of the two half-BD1 motifs appeared to impair, but not completely abolish, the transcriptional activity of CNE-5′JD, suggesting that each half-BD1 motif could be necessary, but not sufficient, to control reporter expression, as observed for the WT BD1. We then concluded that all predicted BD motifs (BD1, BD2, and BD3) are required for the ARX-dependent and -independent *KDM5C* transactivation. To determine whether ARX is able to bind directly to each putative binding site in the CNE-5′JD region, we performed electrophoretic mobility-shift assays (EMSAs) and chromatin-immunoprecipitation (ChIP) experiments. We observed that Myc-tagged ARX bound specifically to the ^{32}P-labeled BD1 and BD2 probes (31-mer) and that those interactions were attenuated by competition with an unlabeled WT template (Figure S3). On the contrary, no band shift was observed with the use of BD3 31-mer, suggesting that this is not a true ARX binding site (Figure S3). Furthermore, using Myc-tagged ARX-expressing SH-SY5Y cells, we found that the BD1 and BD2 fragments were significantly enriched in immunoprecipitation reactions when an Myc antibody was used, but not when an IgG antibody was used (Figure 2A). A weak signal was observed for BD3, whereas no enrichment was observed at the glyceraldehyde-3-phosphate dehidrogenase (*GAPDH* [MIM 138400]) promoter. Quantification of the fold enrichment of the ChIP for each binding site revealed that the BD1 and BD2 regions were enriched at relatively higher levels (3.5-fold and 2.9-fold, respectively), whereas no enrichment signal (1.1-fold) was detected in the BD3 region (Figure 2B). Given that the BD2 and BD3 sites are relatively close to each other and because the sonicated DNA fragments average approximately 500 bp in length, it is possible that the binding to BD2 and BD3 cannot be quantified as an independent event in this assay. Taken together, the luciferase data, bind shift, and ChIP assays suggest that *KDM5C* is undoubtedly a target of ARX, which directly binds to the *KDM5C* BD1 and *KDM5C* BD2 sites with a different efficiency. Instead, it is doubtful that ARX binds, even if only weakly, to the predicted *KDM5C* BD3 site. However, in line with the SI-construct data, the BD3 motif could represent an additional regulatory site required for the recruitment of a specific unknown cofactor that synergizes with ARX to direct *KDM5C* transcription. Interestingly, *KDM5C/Kdm5c* has not been included among the ARX direct-target lists already identified in mice.[35,36] There are several possible explanations for this discrepancy. First, ARX could activate different genetic programs reflecting the functional differences

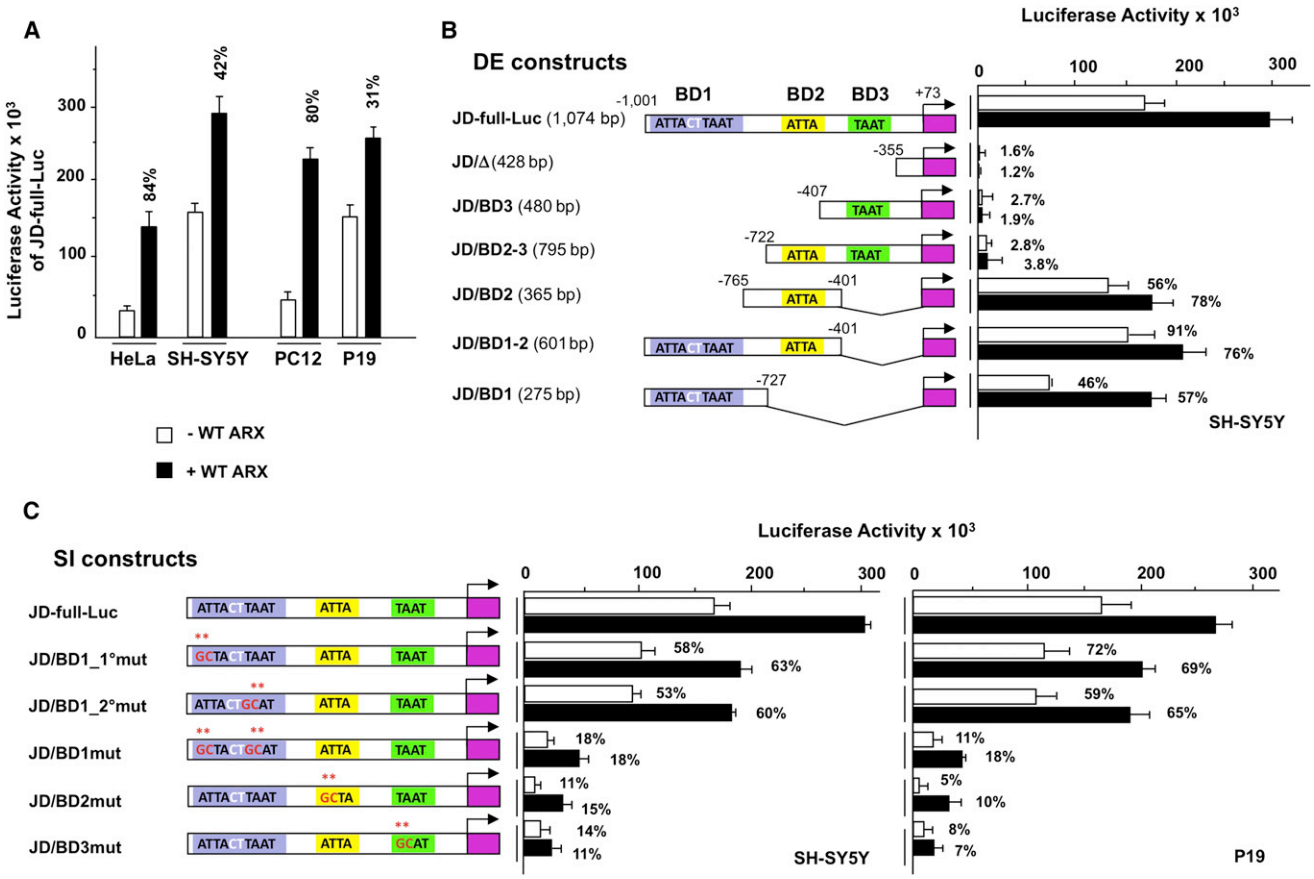

Figure 1. Analysis of the *KDM5C* Regulatory Region, CNE-5′JD, Containing the ARX-Binding Sites

(A) Activity of the WT CNE-5′JD construct (pJD-full-Luc) cotransfected with the WT ARX expression plasmid in human cell lines (HeLa and SH-SY5Y) and rodent cell lines (PC12 and P19). The CNE-5′JD insert is a *KDM5C* fragment (1,074 bp) containing the three predicted ARX-binding sites (BD1, BD2, and BD3), and it was cloned into the pGL3 basic vector (pJD-full-Luc).

(B) Effects of binding-site deletion on the ARX-mediated *KDM5C* transactivation. On the left side is a schematic representation of the WT CNE-5′JD construct and the six luciferase deleted (DE) constructs (pJD/Δ, pJD/BD3, pJD/BD2-3, pJD/BD2, pJD/BD1-2, and pJD/BD1). On the right side is the activity of deleted CNE-5′JD constructs cotransfected with the ARX expression plasmid in SH-SY5Y cells. The DE constructs were obtained by the selective elimination of one or more binding-site modules at a time or by the inclusion of different combinations of a few of them: pJD/Δ was obtained by the digestion of the pJD-full-Luc construct with the restriction enzyme SmaI, and the others were obtained with the use of the genomic clone pJD-full-Luc as a template in PCR reactions.

(C) Effects of binding-site mutagenesis on the ARX-mediated *KDM5C* transactivation: alterations in BD1, BD2, and BD3 nullify the basal and ARX-transactivated CNE-5′JD activity. On the left side is a schematic representation of the WT CNE-5′JD construct and the five luciferase site-directed altered constructs (pJD/BD1_1°mut, pJD/BD1_2°mut, pJD/BD1mut, pJD/BD2mut, and pJD/BD3mut). On the right side is the activity of binding-site-directed CNE-5′JD mutants cotransfected with the ARX expression plasmid in SH-SY5Y and P19 cells. The BD1 palindromic motif 5′-ATTACTTAAT-3′ was mutated into 5′-GCTACTTAAT-3′ (pJD/BD1_1°mut), 5′-ATTACTGCAT-3′ (pJD/BD1_2°mut), and 5′-GCTACTGCAT-3′ (pJD/BD1mut); the BD2 motif 5′-ATTA-3′ was mutated into 5′-GCTA-3′ (pJD/BD2mut); and the BD3 motif 5′-TAAT-3′ was mutated into 5′-GCAT-3′ (pJD/BD3mut).

Cell transient transfections were performed according to standard methods. The primer pairs used for generating the constructs are shown in Table S1. All constructs were verified by DNA sequencing. The reporter activities were measured with the Dual-Luciferase Reporter Assay System (Promega). Each assay was performed in duplicate in three independent experiments, and the resulting firefly-luciferase values were normalized with the renilla values. The activity of the CNE-5′JD construct and each deleted and binding-site-directed mutant transactivated by ARX is reported as a percentage of the expression of the basal JD-full-Luc activity. The error bars express the mean ± SEM.

between the human brain and the mouse brain. Another obvious explanation might be that ARX could act differently depending on the developmental stage, the tissue, and/or the cell-specific context.

Once we had revealed that ARX transactivates the 5′ *KDM5C* regulatory element by binding to the two "TAAT/ATTA" boxes (BD1 and BD2), we found a range of functional deficiencies associated with the ARX polyA elongations, which significantly impair and/or exert interfering effects on the ARX-*KDM5C* interaction. The five mutants tested constitute a specific class of *ARX* (RefSeq NM_139058.2; reference genome build 36) mutations that are associated with a peculiar spectrum of diseases related to XLID and/or epilepsy (Table 1). Of these, the c.333_334ins$(GCG)_7$ (p.Ala109_Ala115dup), c.298_330dup33 (p.Ala105_Ala115dup), and c.430_456dup27 (p.Ala147_Ala155dup) mutations are associated with the most severe forms of epilepsy, whereas the

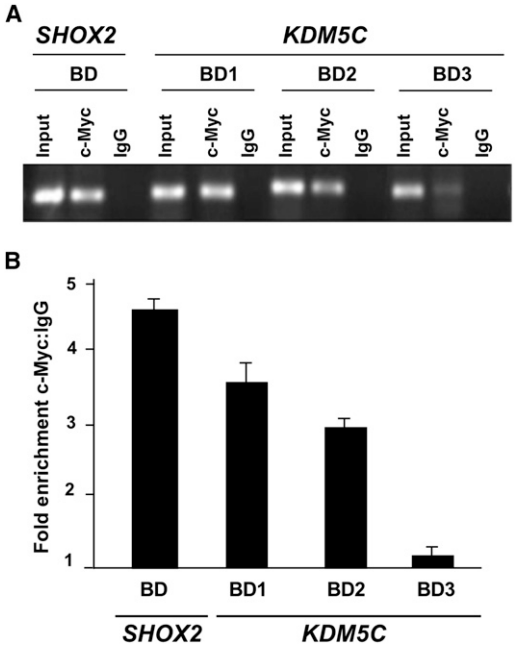

Figure 2. In Vitro Interaction of ARX with the *KDM5C* Regulatory Region

(A) ChIP assay on chromatin from SH-SY5Y cells transfected with Myc-tagged WT ARX. A total of 1×10^7 cells were transfected, and 24 hr after transfection, chromatin was isolated as previously described.[35] The soluble chromatin fraction was incubated with 5 μg of c-Myc antibody (Sigma-Aldrich) or with the control IgG antibody (Santa Cruz Biotechnology) at 4°C overnight. *KDM5C* fragments were PCR amplified with the ChIP primers reported in Table S2. An amplification of the highly conserved *SHOX2/Shox2* binding site was used as a ChIP positive control.[35]

(B) Quantification of the fold enrichment of the ChIP for each binding site located in the *cis*-regulatory region of *KDM5C*. Amplicons were determined with the Power SYBR Green PCR Master Mix (Applied Biosystems) on the 7900HT Fast Real Time PCR System (Applied Biosystems) with the use of a *SHOX2/Shox2* promoter as a positive control[35] and a *GAPDH* promoter as a negative control. The reactions were performed in triplicate in two independent experiments, and a student's t test was used for statistical analysis. The amount of the product was determined relative to a standard curve of input chromatin. The error bars express the mean ± SEM.

c.429_452dup24 (p.Ala148_Ala155dup) and c.423_455 dup33 (p.Gly143_Ala153dup) mutations are present in individuals with mild XLID or epileptic symptoms (Table 1). In SH-SY5Y cotransfection assays, we found a robust reduction of ARX-mediated CNE-5'JD activation in the plasmid JD-full-Luc for three out of five expanded polyA constructs (Figure 3A): c.333_334ins$(GCG)_7$ (p.Ala109_Ala115dup) (63% of the WT ARX construct), c.298_330dup33 (p.Ala105_Ala115dup) (39%), and c.430_456dup27 (p.Ala147_Ala155dup) (56%). The remaining two mutants—those with c.429_452dup24 (p.Ala148_Ala155 dup) and c.423_455dup33 (p.Gly143_Ala153dup)—showed slightly lower (84% and 74%, respectively) luciferase activity than did the WT (Figure 3A). Immunoblot analysis of the transfected cell lysates confirmed that the protein level was equal in all ARX mutants (data not shown).

Table 1. *ARX* Trinucleotide Repeat Expansions and PolyA Elongations in XLID Syndromes and Malignant Epilepsy

DNA Mutation	Protein Alteration	Alanine Elongation[a]	Origin	Disease Severity	Pathology	Seizure	Knockin Model
c.333_334ins$(GCG)_7$	p.Ala109_Ala115dup	[PAI-dup21$_{(7Ala)}$][b]	meiotic de novo	severe	X-linked infantile spasms (West syndrome),[12,24] West syndrome with dystonia;[4,25] severe epileptic dyskinetic encephalopathy[23]	infantile spasms; subclinical spasms; atypical hypsarrhythmia	*Arx*$(GCG)_7$/Y[7]
c.298_330dup33	p.Ala105_Ala115dup	[PAI-dup33$_{(11Ala)}$][b]	meiotic de novo	very severe	Ohtahara syndrome; early infantile epileptic encephalopathy[3]	tonic spasms	-
c.429_452dup24	p.Ala148_Ala155dup	[PAII-dup24$_{(8Ala)}$][c]	meiotic postmitotic mosaicism	variable	syndromic and nonsyndromic ID with or without epilepsy;[12,15,19,20,22] Partington syndrome;[18] X-linked West syndrome with infantile spasms[12,18]	infantile spam convulsions; tonic-clinic seizure; complex partial seizure	*Arx*dup24/Y[7]
c.423_455dup33	p.Gly143_Ala153dup	[PAII-dup33$_{(10Ala+1Gly)}$][c]	meiotic de novo	variable	ID with epilepsy and distonia and intermittent hyperventilation[26]	epilepsy with rare generalized spike and wave activity	-
c.430_456dup27	p.Ala147_Ala155dup	[PAII-dup27$_{(9Ala)}$][c]	postmitotic mosaicism	severe	X-linked infantile spasms (West syndrome); death early in the life[27]	infantile spasm convulsions	-

The following abbreviation is used: ID, intellectual disability.
[a]In this column, aliases of ARX alterations are shown in brackets.
[b]The WT polyA length is PolyA I(Ala)16.
[c]The WT polyA length is PolyA II(Ala)12.

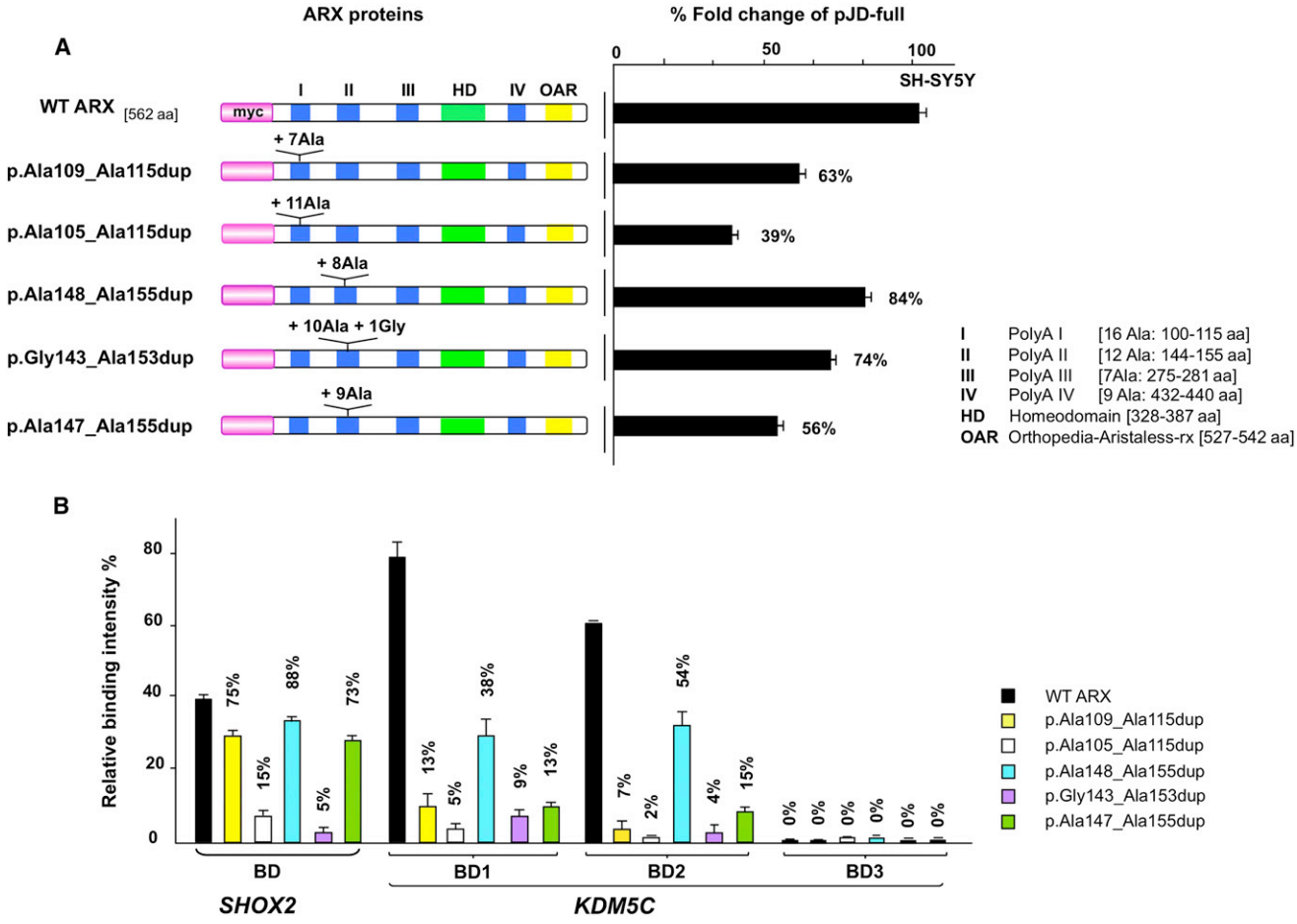

Figure 3. Impact of WT ARX and ARX PolyA Elongations on the *cis*-Regulating Element of *KDM5C*
(A) Cotransfection experiments of ARX polyA elongations with the *KDM5C* 5′ region in SH-SY5Y cells (pJD-full-Luc). On the left side is a schematic representation of the WT ARX and the five polyA elongations studied; two of them (p.Ala109_Ala115dup and p.Ala105_Ala115dup) fall within the first polyA tract, and the remaining three (p.Ala148_Ala155dup, p.Gly143_Ala153dup, and p.Ala147_Ala155dup) fall within the second polyA tract. Alanine insertions are shown for each mutant. On the right side is the activity of the CNE-5′JD element transactivated by the WT ARX and ARX polyA mutants. For each assay, four independent experiments were performed in triplicate. The activity of each mutated construct is reported as a percentage of the expression of the basal pJD-full-Luc activity. The error bars express the mean ± SEM.
(B) Phosphoimager analysis of the EMSA results. A Typhoon 9200 scanner (GE Healthcare) was used for analyzing the EMSA gels.[39] The bands corresponding to the bindings were analyzed with ImageQuant 5.0 software. The results are represented as a mean intensity relative to the free oligo band. Quantification of the data is presented as averages. SDs were established in two independent measurements. The binding intensity of each mutated construct is reported as a percentage of the binding intensity of the WT ARX. The error bars express the mean ± SEM.

Given that we had established that alanine expansions impair ARX stimulation of the *KDM5C* regulatory element in SH-SY5Y cells, we hypothesized that those mutations might also reduce the binding of ARX. Therefore, to test this hypothesis, we carried out EMSA and ChIP experiments by using the three predicted *KDM5C* sites as ARX targets, as well as the Myc-tagged altered ARX proteins containing either the WT sequence or the polyA I and polyA II elongations. EMSAs revealed that, compared to WT ARX, the polyA alterations produce reduced ARX DNA-binding activity at both BD1 and BD2; however, no band shift was observed with the BD3 31-mer, as expected (Figure S4). In particular, the c.298_330dup33 (p.Ala105_Ala115dup) mutation produced a more evident binding reduction at both BD1 and BD2; the reductions caused by c.333_334ins$(GCG)_7$ (p.Ala109_Ala115dup), c.423_455dup33 (p.Gly143_Ala153dup), and c.430_456dup27 (p.Ala147_Ala155dup) were less evident (Figure S4). On the contrary, compared to the WT ARX, c.429_452dup24 (p.Ala148_Ala155dup) showed a higher DNA binding activity than did the other mutations at both BD1 and BD2 sites, as well as an unexpected increased affinity to BD2 (Figure S4). The shifted bands were quantified by phosphorimager analysis (Figure 3B), which showed an overall binding defect that can be ranked as follows: c.298_330dup33 > c.430_456dup27 > c.333_334ins$(GCG)_7$ > c.423_455dup33 > c.429_452dup24.

The altered recruitment of the ARX polyA mutants was also verified by ChIP assay with chromatin from transfected SH-SY5Y cells. We found that the polyA proteins,

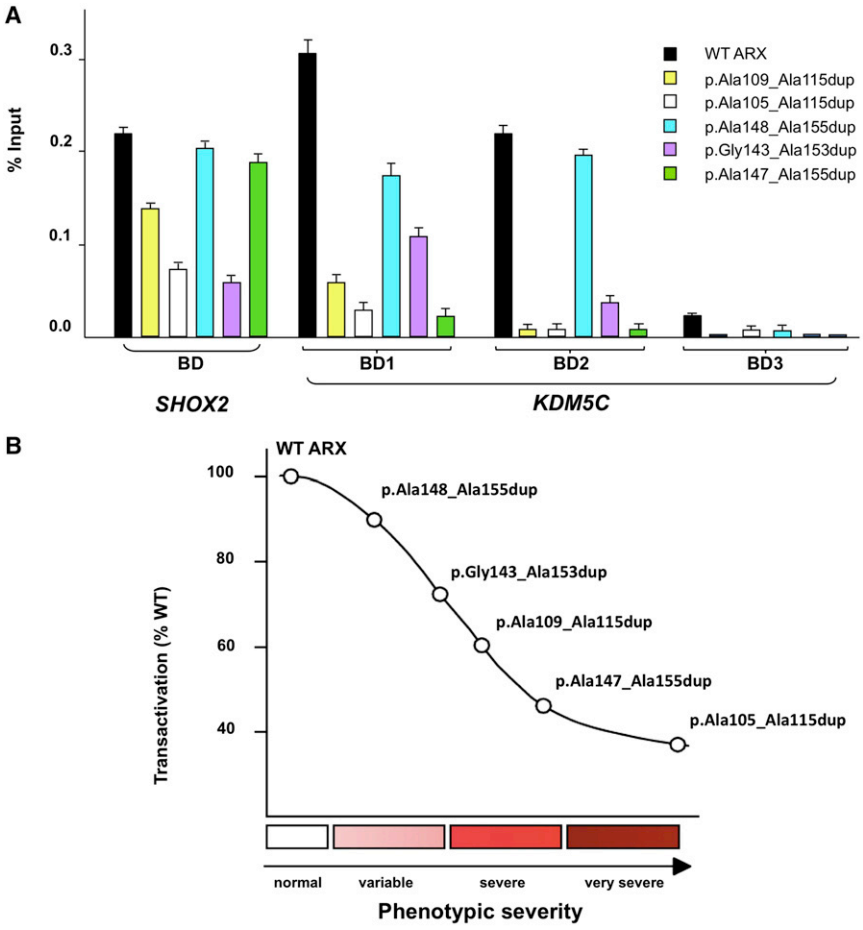

Figure 4. Defects of ARX PolyA Elongations

(A) ChIP enrichments of the *KDM5C* BD1, BD2, and BD3 regions with the use of either the WT ARX or the polyA-expanded immunoprecipitates. The DNA was extracted, and fragments of the three predicted ARX-binding sites were PCR amplified with *KDM5C* ChIP primers. All values were normalized to the corresponding input control sample. The reactions were performed in triplicate in two independent experiments, and a student's t test was used for statistical analysis. The error bars express the mean ± SEM.

(B) ARX polyA alterations with different in vitro functional consequences mirror the spectrum of developmental defects observed in XLID and epilepsy individuals. *KDM5C* transactivation data as a function of the degree of severity of the ARX polyA subphenotypes (variable, severe, and very severe) were fitted to an S-shaped curve. The plot was generated by a comparison of the c.333_334ins $(GCG)_7$ (p.Ala109_Ala115dup), c.298_330 dup33 (p.Ala105_Ala115dup), c.429_452 dup24 (p.Ala148_Ala155dup), c.423_455 dup33 (p.Gly143_Ala153dup), and c.430_456dup27 (p.Ala147_Ala155dup) mutant activity.

severely defective for EMSA binding, exhibited a decreased chromatin binding to the *KDM5C* BD1 and BD2 sites (Figure 4A). Low-background binding signals were detected in the ChIP assays for IgG (data not shown). As expected, the c.429_452dup24 (p.Ala148_Ala155dup) mutation showed less severe chromatin-binding defects with respect to BD1 and BD2 than did the other elongation mutations. The c.298_330dup33 (p.Ala105_Ala115dup), c.333_334ins$(GCG)_7$ (p.Ala109_Ala115dup), c.423_455dup33 (p.Gly143_Ala153dup), and c.430_456 dup27 (p.Ala147_Ala155dup) mutants were defective for BD1 binding but showed a more detrimental defect for BD2. Quite strikingly, we found that the ARX polyA alterations slightly impair the binding to a well-known ARX target, *SHOX2/Shox2*[28,31,35] (Figure 3B and 4A), which has a crucial role in a different tissue-specific developmental program.[40] This points to the possibility that the polyA-defect severity might depend on the ARX-target promoter context used. Collectively, our in vitro studies imply a differential impairment of the ARX-*KDM5C* interaction mediated by the polyA elongations in ARX. We therefore hypothesize that three out of the five mutations, c.298_330dup33 (p.Ala105_Ala115dup), c.333_334ins$(GCG)_7$ (p.Ala109_Ala115dup), and c.430_456dup27 (p.Ala147_Ala155dup), which result in severe *KDM5C* defects in vitro (Table 2), might cause a severe effect on *KDM5C* in vivo. Interestingly, the individuals carrying the c.298_330dup33 (p.Ala105_Ala115dup), c.333_334ins $(GCG)_7$ (p.Ala109_Ala115dup), or c.430_456dup27 (p.Ala147_Ala155dup) mutations showed malignant epilepsy, which is often associated with brain malformations (Table 1). The remaining two mutations, c.429_452dup24 (p.Ala148_Ala155dup) and c.423_455dup33 (p.Gly143_Ala153dup), which are associated with less severe phenotypes, result in a much less striking reduction in the transactivation and binding to *KDM5C* BD1 and BD2 (Table 2), as well as to the *SHOX2/Shox2* binding site. We therefore exclude a correlation between the *KDM5C* defects and the length of the cotransfected polyA tracts and instead propose a link between the spectrum of the polyA-related defects and the severity of the outcomes associated with XLID and/or epilepsy. Consequently, we can classify the ARX polyA elongations as hypomorphic alterations causing a partial loss of function of ARX, a conclusion that fits well with the observation that the human phenotypes resulting from c.429_452dup24 (p.Ala148_Ala155dup) or c.423_455dup33 (p.Gly143_Ala153dup) lie at the milder end of the phenotypic spectrum of XLID and/or epilepsy than do those resulting from other types of ARX polyA elongations.[9,12,15] In Figure 4B, we illustrate our understanding of how the interaction between the polyA alterations and *KDM5C* determines the phenotypic complexity in response to hypomorphic ARX activity. If we consider the molecular

Table 2. *KDM5C* Defects and ARX Cellular Localization Associated with ARX PolyA-Expansion Alterations

	Functional Defect			
Elongated Protein	***KDM5C* Transactivation[a]**	**BD1 Binding[a]**	**BD2 Binding[a]**	**ARX Localization**
p.Ala109_Ala115dup	63%	20%	9%	nuclear and cytoplasmatic
p.Ala105_Ala115dup	39%	13%	9%	nuclear with inclusions
p.Ala148_Ala155dup	84%	60%	87%	nuclear
p.Gly143_Ala153dup	74%	43%	22%	nuclear with inclusions
p.Ala147_Ala155dup	56%	7%	4%	nuclear and cytoplasmatic with inclusions

[a]The percentages in these columns are compared to the WT protein.

effects of each alteration, we can display their functional defects along a spectrum of subphenotypes passed through a sigmoid (S-shaped) curve: the lower the ARX polyA activity, the more severe the phenotype of XLID and/or epilepsy. Accordingly, we anticipate that XLID and/or epilepsy hemizygous males with hypomorphic ARX polyA alterations could have a partial or low level of residual ARX activity, whereas carrier females are generally asymptomatic or present with very mild neurological symptoms,[1,2,15] as expected in the case of disease alleles associated with random X-inactivation phenomena.

The molecular mechanisms responsible for the reduced binding and transactivation are still enigmatic. A reduced DNA binding and declined transactivation activity could be the consequence of an abnormal folding and spontaneous aggregation of the altered proteins. Indeed, homopolymeric-expansion diseases, such as those associated with polyA or polyglutammine expansions, can be classified as "protein-misfolding disorders" because the altered proteins do not fold stably into their normal functional shape and then aggregate.[16]

As expected, transient transfection of WT and altered ARX in SH-SY5Y cells confirmed[21,29,30] that, except for the c.429_452dup24 (p.Ala148_Ala155 dup) mutant, the other tested polyA mutants mislocalize and form apparent insoluble cytoplasmatic and/or nuclear aggregates (Figure S5); this might prevent ARX from entering the nucleus and exerting its function on *KDM5C*. A similar situation has been reported in the study of polyA expansions in zinc-finger protein of cerebellum 2 (*ZIC2* [MIM 603073]), associated with holoprosencephaly (MIM 609637),[41] and in paired-like homeobox 2B (*PHOX2B* [MIM 603851]), associated with central hypoventilation syndrome (MIM 209880).[42] Surprisingly, no specific ARX aggregation was noted in the mouse model carrying either c.333_334ins$(GCG)_7$[7,8,31] or c.429_452 dup24,[7] even if a cytoplasmatic localization greater than that of the WT protein was detected in the neurons expressing c.333_334ins$(GCG)_7$.[8] Another obvious explanation for the reduced *KDM5C* activation is that the alanine-tract expansions disturb the interaction between ARX and an essential cofactor, as recently hypothesized in a study of the mouse model carrying c.333_334ins$(GCG)_7$.[31] On the other hand, apart from BD1 and BD2, which are both necessary for driving the ARX-dependent transactivation of *KDM5C*, BD3 seems to be related to basal *KDM5C* expression. Therefore, ARX could synergize with another regulatory protein in the activation of *KDM5C* transcription, as already detected during murine myogenesis in the ARX-dependent activation of MADS-box transcription-enhancer factor 2, polypeptide C (*Mef2C* [MIM 600662]) expression.[43] In both hypotheses, the functional outcome could be an abnormal ARX recruitment to the *KDM5C* regulatory element and perhaps to other promoter targets. This phenomenon could explain the partial loss of activity shown by the polyA-elongated altered versions of ARX on the *KDM5C* and *SHOX2* regulatory elements.

Because we hypothesized that *KDM5C* is a direct positive target of ARX, we sought to investigate whether murine *Kdm5c* expression is affected by the absence of ARX. A large body of evidence indicates that both ARX and KDM5C are needed in the early phases of murine embryo development and in the differentiated neuronal cells.[33,34,44–48] Murine embryonic in-situ-hybridization studies have revealed that *Arx* is expressed at a very early stage and that a weak signal is detectable at the 3-somite stage (when the neural plate is defined) and that a strong signal is detectable at the 10-somite stage in the dorsal murine telencephalon regions.[45] It has been reported that KDM5C is essential for notochord development[33,44] and dendrite arborization.[49] Given that the XLID- and/or epilepsy-associated mutations in *ARX* or *KDM5C* might affect the GABAergic functions, we studied the temporal and quantitative patterns of the emergence of *Kdm5c* mRNA in WT and *Arx*-knockout (KO) embryonic stem (ES) cells during in vitro neuronal differentiation. We applied a protocol allowing primarily GABAergic neuron formation, an in vitro method that recapitulates the expression patterns and developmental processes of neurogenesis.[50] The mRNA expression of the murine counterparts of *KDM5C* (*Kdm5c* [RefSeq NM_013668.3]) and *ARX* (*Arx* [RefSeq NC_000086.6]) were measured by quantitative RT-PCR. In the WT in vitro neuronal model, the coexpression of *Arx* and *Kdm5c* became evident at the developmental transitions between day 8 and day 10 and reached higher levels in the fully differentiated ES cells than in the

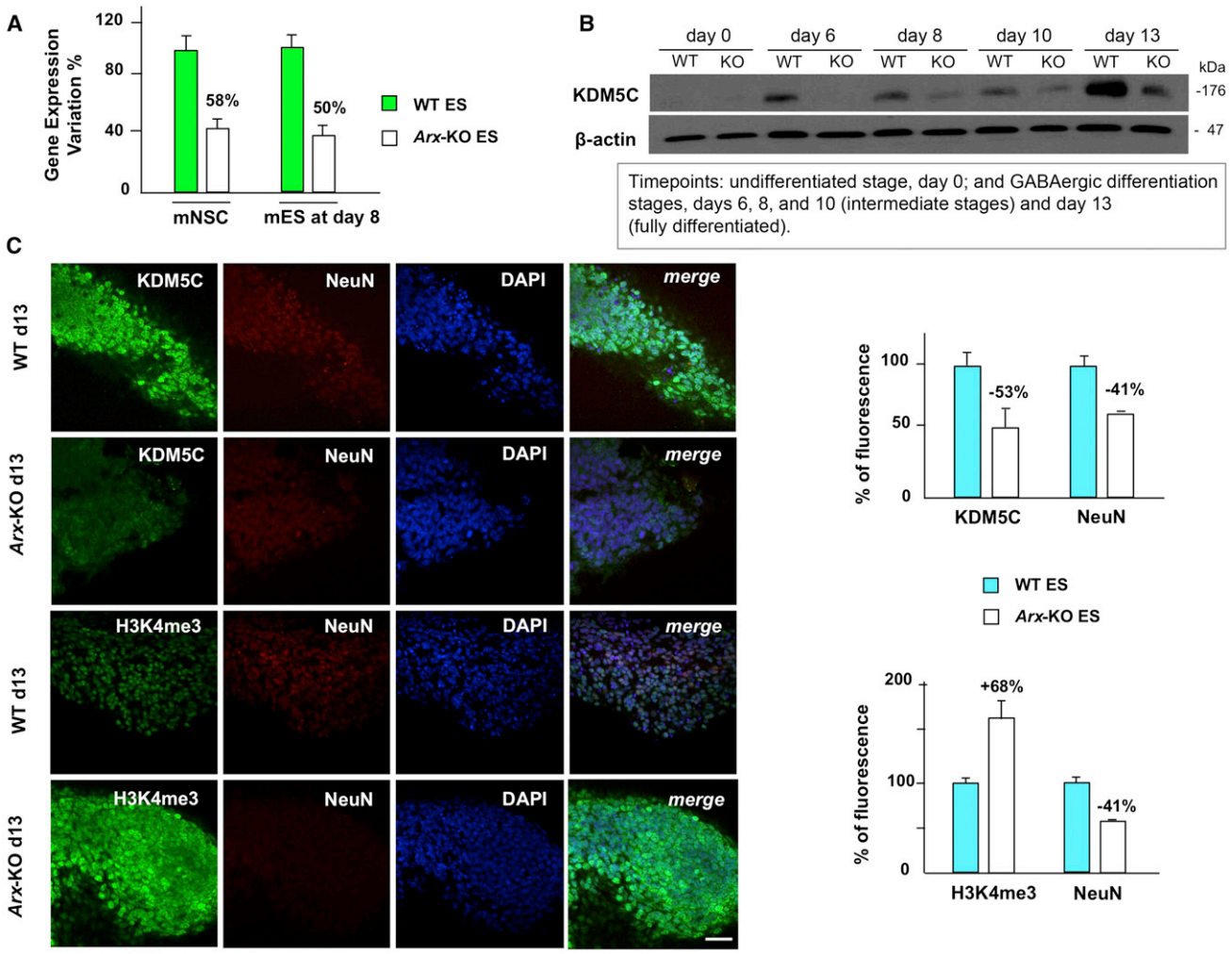

Figure 5. Downregulation of *Kdm5c*/KDM5C in Neuronal Cells Derived from *Arx*-KO ES Cells

(A) Real-time-PCR analysis of the *Kdm5c* transcript in *Arx*-KO mouse neural stem cells (NSCs) and *Arx*-KO mouse ES cells differentiated in neuronal cells. The NSCs from the WT and *Arx*-KO mice[51] were cultured in DMEM-F12.[52] The ES cells derived from the WT male and *Arx*-KO mice[51] were maintained in an undifferentiated state by culture on a monolayer of mitomycin-C-inactivated fibroblasts in the presence of leukemia-inhibiting factor. The culture protocol for neuronal differentiation was carried out as described elsewhere.[50] The total RNA was extracted according to TRIzol protocol (Invitrogen) and was reverse transcribed with the SuperScript III First Strand Synthesis System (Invitrogen). The steady-state mRNA abundance was determined as described elsewhere.[53,54] The primers used for the *Kdm5c* transcript analyses are reported in Table S3. The data were normalized with *Gapdh* and *18S* as control transcripts. The quantity of each transcript compared to that expressing the WT cells is reported as a percentage. For each assay, four independent experiments were performed in triplicate. The error bars express the mean ± SEM.

(B) Immunoblot analysis of KDM5C in *Arx*-KO and WT ES cells at different time points during neuronal differentiation. The cell extracts were prepared and separated as described previously.[50,53] After blocking with 5% nonfat milk, the membranes were incubated with human KDM5C antibody (1:1,000, Santacruz). The β-actin antibody (1:3,000, Santacruz) was used as a loading control. The signals were detected with an enhanced chemiluminescence kit (Amersham Biosciences).

(C) Immunofluorescence analysis of KDM5C and H3K4me3 in ES-cell-derived neuronal cells. The differentiated ES cells were examined for the level of KDM5C (1:50, Santacruz), H3K4me3 (1:3,000, Abcam), and NeuN (1:100, Millipore/Chemicon). Mouse AlexaFluor-488 (1:200, Invitrogen) and Texas Red (1:200, Molecular Probes) were used. The images were superimposed with nuclear DAPI (1:5,000, Roche) staining and taken randomly under a ZEISS confocal microscope. Both the immunopositive cells (KDM5C- or H3K4me3-stained nuclei) and total DAPI-stained nuclei were counted. The fluorescence percentage of immunopositive neuronal cells was calculated as a proportion of the immunopositive NeuN cells. Five fields from three replicates for each marker were analyzed. The activity of the marked protein localized in the WT ES cells compared to that present in the *Arx*-KO ES cells is reported as a percentage decrease (−) or percentage increase (+). Scale bars represent 20 μm, and error bars represent the mean ± SEM.

undifferentiated ES cells (Figure S6A). The coexistence of both transcripts was also proved in embryonic and postnatal human and murine brain tissues (Figure S6B). It is noteworthy that when we tested the *Kdm5c* transcript in *Arx*-KO ES cells at day 8, we observed that its expression was much lower than in WT cells (Figure 5A). A comparable reduction was observed in the free-floating cultures of neural stem cells (NSCs) isolated from the *Arx*-KO brain embryo (Figure 5A). The decrease in *Kdm5c* expression correlates with the decrease in protein levels shown by

immunoblot analysis of cultured GABAergic neurons from *Arx*-KO and WT ES cells (Figure 5B). By immunofluorescence analysis, we also detected the reduced presence of KDM5C in intermediate (data not shown) and fully differentiated cells (Figure 5C). We hypothesize that both genes could be required in a specific time frame of neuronal development and, that, in the absence of ARX, the *Kdm5c* expression might be altered at neural induction and in the following stages until the final terminal differentiation. Furthermore, we have also established that a decrease in KDM5C inversely correlates with an increase in H3K4me3 signaling, potentially as a result of compromised KDM5C activity. Indeed, a detectable alteration in the level of H3K4me3 was observed in NeuN-positive neurons (Figure 5C) and in β-III-tubulin-positive neurons (Figure S7). H3K4me3 is the main KDM5C nucleosomal substrate and the hallmark of the majority of ES promoters. As the ES cells are induced to differentiate along a neuronal cell lineage, specific chromatin-remodeling complexes recognize H3K4me3 and open the chromatin structure to facilitate the transcription of specific promoters.[55] As a result of an abnormality in the KDM5C-H3K4me3 pathway, target genes would be transcribed more abundantly in the *Arx*-KO cells than in the WT cells. Our data are consistent with the H3K4me3 defects observed in association with XLID KDM5C-altered proteins.[34] Noteworthy, it has been proved that XLID KDM5C mutants alter the promoter activity of a subset of REST targets; two such examples are those encoded by genes mutated in children with epilepsy: sodium-channel type 2A (*SCN2A* [MIM 182390]),[49,55] associated with early infantile epileptic encephalopathy-11 (MIM 613721), and synapsin I (*SYN1* [MIM 313440]),[49,55] associated with X-linked epilepsy with variable learning disabilities and behavioral disorders (MIM 300491). These considerations have led to the interesting suggestion that a decrease in KDM5C activity could abrogate or impair REST-mediated neuronal gene regulation, thus contributing to the pathogenesis of ARX-KDM5C-associated XLID and/or epilepsy. One essential question that remains to be answered is the impact of an abnormal ARX-KDM5C-H3K4me3 pathway on neuronal differentiation and how this might contribute to ARX diseases. In the *Arx*-KO cells, we observed abnormalities in the rosette-like formation and neuronal precursor markers, suggesting a delay in achieving full neuronal maturation in vitro (L.P., unpublished data). In summary, we provide here a snapshot of the function of ARX by linking polyA expansions to *KDM5C*, mutations of which cause XLID and/or epilepsy. In this exciting scenario, we propose that the XLID- and/or epilepsy-related diseases in children with ARX polyA alterations might in part be caused by aberrant histone demethylation resulting from a *KDM5C* defect. Various mechanisms by which *ARX* mutations might cause the dysfunction of GABAergic interneurons and might thus result in XLID and epilepsy phenotypes have recently been discussed.[56,57] Our work describes a mechanism that not only expands on the existing hypotheses but implicates another known gene associated with the XLID and/or epilepsy phenotype in *ARX* pathologies, a class of diseases with extremely limited therapeutic options. Because chromatin modifications are reversible, it is possible that epigenetic drugs could compensate for the *ARX*-dependent KDM5C-H3K4me3 deregulation. Even though many other ARX targets could have important roles in the expansion phenotype, a further development of our research could open up the possibility of additional studies aimed at mitigating the symptom severity associated with the ARX polyA neurophenotypes and with many other XLID- and/or epilepsy-related pathologies.

Supplemental Data

Supplemental Data include seven figures and three tables and can be found with this article online at http://www.cell.com/AJHG.

Acknowledgments

The authors would like to thank G. Courtois for the Myc antibody, as well as the Institute of Genetics and Biophysics Consiglio Nazionale delle Ricerche Integrated Microscopy Facility for helping with the microscopy analysis. They also thank P. Miano for assistance with the graphics. This work was supported by the Juvenile Diabetes Research Foundation (17-2011-16, 2-2010-567, 26-2008-639), the Institut National de la Santé et de la Recherche Médicale AVENIR program, and the European Research Council (StG-2011-281265) to P.C.; by grants from the National Health and Medical Research Council of Australia to J.G. (project grant 1008077 and principal research fellowship 508043) and to C.S. (project grant 1002732 and the M.S. McLeod Fellowship); by a Foundation Telethon grant to M.V.U.; and by a Fondation Jérôme Lejeune grant to M.G.M.

Received: May 10, 2012
Revised: June 7, 2012
Accepted: November 13, 2012
Published: December 13, 2012

Web Resources

The URLs for data presented herein are as follows:

Ensembl Genome Browser, http://www.ensembl.org/
GenBank, http://www.ncbi.nih.gov/Genbank/
Genomatix, http://www.genomatix.de
Online Mendelian Inheritance in Man (OMIM), http://www.omim.org
TRANSFAC Transcription Factor Binding Sites, http://www.biobase-international.com/product/transcription-factor-binding-sites
UCSC Genome Browser, http://www.genome.ucsc.edu
VISTA, http://genome.lbl.gov/vista/index.shtml

References

1. Gécz, J., Cloosterman, D., and Partington, M. (2006). ARX: A gene for all seasons. Curr. Opin. Genet. Dev. *16*, 308–316.

2. Shoubridge, C., Fullston, T., and Gécz, J. (2010). ARX spectrum disorders: Making inroads into the molecular pathology. Hum. Mutat. *31*, 889–900.
3. Kato, M., Saitoh, S., Kamei, A., Shiraishi, H., Ueda, Y., Akasaka, M., Tohyama, J., Akasaka, N., and Hayasaka, K. (2007). A longer polyalanine expansion mutation in the ARX gene causes early infantile epileptic encephalopathy with suppression-burst pattern (Ohtahara syndrome). Am. J. Hum. Genet. *81*, 361–366.
4. Poirier, K., Eisermann, M., Caubel, I., Kaminska, A., Peudonnier, S., Boddaert, N., Saillour, Y., Dulac, O., Souville, I., Beldjord, C., et al. (2008). Combination of infantile spasms, non-epileptic seizures and complex movement disorder: A new case of ARX-related epilepsy. Epilepsy Res. *80*, 224–228.
5. Kato, M., Das, S., Petras, K., Kitamura, K., Morohashi, K., Abuelo, D.N., Barr, M., Bonneau, D., Brady, A.F., Carpenter, N.J., et al. (2004). Mutations of ARX are associated with striking pleiotropy and consistent genotype-phenotype correlation. Hum. Mutat. *23*, 147–159.
6. Friocourt, G., and Parnavelas, J.G. (2010). Mutations in ARX Result in Several Defects Involving GABAergic Neurons. Front Cell Neurosci. *4*, 4–14.
7. Kitamura, K., Itou, Y., Yanazawa, M., Ohsawa, M., Suzuki-Migishima, R., Umeki, Y., Hohjoh, H., Yanagawa, Y., Shinba, T., Itoh, M., et al. (2009). Three human ARX mutations cause the lissencephaly-like and mental retardation with epilepsy-like pleiotropic phenotypes in mice. Hum. Mol. Genet. *18*, 3708–3724.
8. Price, M.G., Yoo, J.W., Burgess, D.L., Deng, F., Hrachovy, R.A., Frost, J.D., Jr., and Noebels, J.L. (2009). A triplet repeat expansion genetic mouse model of infantile spasms syndrome, Arx(GCG)10+7, with interneuronopathy, spasms in infancy, persistent seizures, and adult cognitive and behavioral impairment. J. Neurosci. *29*, 8752–8763.
9. Strømme, P., Mangelsdorf, M.E., Scheffer, I.E., and Gécz, J. (2002). Infantile spasms, dystonia, and other X-linked phenotypes caused by mutations in Aristaless related homeobox gene, ARX. Brain Dev. *24*, 266–268.
10. Bienvenu, T., Poirier, K., Friocourt, G., Bahi, N., Beaumont, D., Fauchereau, F., Ben Jeema, L., Zemni, R., Vinet, M.C., Francis, F., et al. (2002). ARX, a novel Prd-class-homeobox gene highly expressed in the telencephalon, is mutated in X-linked mental retardation. Hum. Mol. Genet. *11*, 981–991.
11. Kitamura, K., Yanazawa, M., Sugiyama, N., Miura, H., Iizuka-Kogo, A., Kusaka, M., Omichi, K., Suzuki, R., Kato-Fukui, Y., Kamiirisa, K., et al. (2002). Mutation of ARX causes abnormal development of forebrain and testes in mice and X-linked lissencephaly with abnormal genitalia in humans. Nat. Genet. *32*, 359–369.
12. Strømme, P., Mangelsdorf, M.E., Shaw, M.A., Lower, K.M., Lewis, S.M., Bruyere, H., Lütcherath, V., Gedeon, A.K., Wallace, R.H., Scheffer, I.E., et al. (2002). Mutations in the human ortholog of Aristaless cause X-linked mental retardation and epilepsy. Nat. Genet. *30*, 441–445.
13. Kato, M., and Dobyns, W.B. (2005). X-linked lissencephaly with abnormal genitalia as a tangential migration disorder causing intractable epilepsy: Proposal for a new term, "interneuronopathy". J. Child Neurol. *20*, 392–397.
14. Miano, M.G., Laperuta, C., and Ursini, M.V. (2007). From Nonsyndromic X-linked Mental Retardation (MRX) diseases to discovery genes for cognitive circuitry in humans. In Focus on Medical Genetics and Down's Syndrome Research, R.A. Firthel, ed. (Hauppauge, New York: Nova Science Publishers), pp. 1–49.
15. Laperuta, C., Spizzichino, L., D'Adamo, P., Monfregola, J., Maiorino, A., D'Eustacchio, A., Ventruto, V., Neri, G., D'Urso, M., Chiurazzi, P., et al. (2007). MRX87 family with Aristaless X dup24bp mutation and implication for polyalanine expansions. BMC Med. Genet. *8*, 25.
16. López Castel, A., Cleary, J.D., and Pearson, C.E. (2010). Repeat instability as the basis for human diseases and as a potential target for therapy. Nat. Rev. Mol. Cell Biol. *11*, 165–170.
17. Conti, V., Marini, C., Mei, D., Falchi, M., Ferrari, A.R., and Guerrini, R. (2011). Contractions in the second polyA tract of ARX are rare, non-pathogenic polymorphisms. Am. J. Med. Genet. A. *155A*, 164–167.
18. Partington, M.W., Turner, G., Boyle, J., and Gécz, J. (2004). Three new families with X-linked mental retardation caused by the 428-451dup(24bp) mutation in ARX. Clin. Genet. *66*, 39–45.
19. Poirier, K., Abriol, J., Souville, I., Laroche-Raynaud, C., Beldjord, C., Gilbert, B., Chelly, J., and Bienvenu, T. (2005). Maternal mosaicism for mutations in the ARX gene in a family with X linked mental retardation. Hum. Genet. *118*, 45–48.
20. Stepp, M.L., Cason, A.L., Finnis, M., Mangelsdorf, M., Holinski-Feder, E., Macgregor, D., MacMillan, A., Holden, J.J., Gecz, J., Stevenson, R.E., and Schwartz, C.E. (2005). XLMR in MRX families 29, 32, 33 and 38 results from the dup24 mutation in the ARX (Aristaless related homeobox) gene. BMC Med. Genet. *6*, 16.
21. Fullston, T., Finnis, M., Hackett, A., Hodgson, B., Brueton, L., Baynam, G., Norman, A., Reish, O., Shoubridge, C., and Gecz, J. (2011). Screening and cell-based assessment of mutations in the Aristaless-related homeobox (ARX) gene. Clin. Genet. *80*, 510–522.
22. Van Esch, H., Poirier, K., de Zegher, F., Holvoet, M., Bienvenu, T., Chelly, J., Devriendt, K., and Fryns, J.P. (2004). ARX mutation in a boy with transsphenoidal encephalocele and hypopituitarism. Clin. Genet. *65*, 503–505.
23. Guerrini, R., Moro, F., Kato, M., Barkovich, A.J., Shiihara, T., McShane, M.A., Hurst, J., Loi, M., Tohyama, J., Norci, V., et al. (2007). Expansion of the first PolyA tract of ARX causes infantile spasms and status dystonicus. Neurology *69*, 427–433.
24. Shinozaki, Y., Osawa, M., Sakuma, H., Komaki, H., Nakagawa, E., Sugai, K., Sasaki, M., and Goto, Y. (2009). Expansion of the first polyalanine tract of the ARX gene in a boy presenting with generalized dystonia in the absence of infantile spasms. Brain Dev. *31*, 469–472.
25. Cossée, M., Faivre, L., Philippe, C., Hichri, H., de Saint-Martin, A., Laugel, V., Bahi-Buisson, N., Lemaitre, J.F., Leheup, B., Delobel, B., et al. (2011). ARX polyalanine expansions are highly implicated in familial cases of mental retardation with infantile epilepsy and/or hand dystonia. Am. J. Med. Genet. A. *155A*, 98–105.
26. Demos, M.K., Fullston, T., Partington, M.W., Gécz, J., and Gibson, W.T. (2009). Clinical study of two brothers with a novel 33 bp duplication in the ARX gene. Am. J. Med. Genet. A. *149A*, 1482–1486.
27. Reish, O., Fullston, T., Regev, M., Heyman, E., and Gecz, J. (2009). A novel de novo 27 bp duplication of the ARX gene, resulting from postzygotic mosaicism and leading to three

severely affected males in two generations. Am. J. Med. Genet. A. *149A*, 1655–1660.

28. Shoubridge, C., Tan, M.H., Seiboth, G., and Gécz, J. (2012). ARX homeodomain mutations abolish DNA binding and lead to a loss of transcriptional repression. Hum. Mol. Genet. *21*, 1639–1647.
29. Nasrallah, I.M., Minarcik, J.C., and Golden, J.A. (2004). A polyalanine tract expansion in Arx forms intranuclear inclusions and results in increased cell death. J. Cell Biol. *167*, 411–416.
30. Shoubridge, C., Cloosterman, D., Parkinson-Lawerence, E., Brooks, D., and Gécz, J. (2007). Molecular pathology of expanded polyalanine tract mutations in the Aristaless-related homeobox gene. Genomics *90*, 59–71.
31. Nasrallah, M.P., Cho, G., Simonet, J.C., Putt, M.E., Kitamura, K., and Golden, J.A. (2012). Differential effects of a polyalanine tract expansion in Arx on neural development and gene expression. Hum. Mol. Genet. *21*, 1090–1098.
32. Jensen, L.R., Amende, M., Gurok, U., Moser, B., Gimmel, V., Tzschach, A., Janecke, A.R., Tariverdian, G., Chelly, J., Fryns, J.P., et al. (2005). Mutations in the JARID1C gene, which is involved in transcriptional regulation and chromatin remodeling, cause X-linked mental retardation. Am. J. Hum. Genet. *76*, 227–236.
33. Jensen, L.R., Bartenschlager, H., Rujirabanjerd, S., Tzschach, A., Nümann, A., Janecke, A.R., Spörle, R., Stricker, S., Raynaud, M., Nelson, J., et al. (2010). A distinctive gene expression fingerprint in mentally retarded male patients reflects disease-causing defects in the histone demethylase KDM5C. Pathogenetics *3*, 2.
34. Iwase, S., Lan, F., Bayliss, P., de la Torre-Ubieta, L., Huarte, M., Qi, H.H., Whetstine, J.R., Bonni, A., Roberts, T.M., and Shi, Y. (2007). The X-linked mental retardation gene SMCX/JARID1C defines a family of histone H3 lysine 4 demethylases. Cell *128*, 1077–1088.
35. Fulp, C.T., Cho, G., Marsh, E.D., Nasrallah, I.M., Labosky, P.A., and Golden, J.A. (2008). Identification of Arx transcriptional targets in the developing basal forebrain. Hum. Mol. Genet. *17*, 3740–3760.
36. Quillé, M.L., Carat, S., Quéméner-Redon, S., Hirchaud, E., Baron, D., Benech, C., Guihot, J., Placet, M., Mignen, O., Férec, C., et al. (2011). High-throughput analysis of promoter occupancy reveals new targets for Arx, a gene mutated in mental retardation and interneuronopathies. PLoS ONE *6*, e25181.
37. Shoubridge, C., Tarpey, P.S., Abidi, F., Ramsden, S.L., Rujirabanjerd, S., Murphy, J.A., Boyle, J., Shaw, M., Gardner, A., Proos, A., et al. (2010). Mutations in the guanine nucleotide exchange factor gene IQSEC2 cause nonsyndromic intellectual disability. Nat. Genet. *42*, 486–488.
38. Wilson, D., Sheng, G., Lecuit, T., Dostatni, N., and Desplan, C. (1993). Cooperative dimerization of paired class homeo domains on DNA. Genes Dev. *7*, 2120–2134.
39. Chen, S., Wang, Q.L., Xu, S., Liu, I., Li, L.Y., Wang, Y., and Zack, D.J. (2002). Functional analysis of cone-rod homeobox (CRX) mutations associated with retinal dystrophy. Hum. Mol. Genet. *11*, 873–884.
40. Liu, H., Chen, C.H., Espinoza-Lewis, R.A., Jiao, Z., Sheu, I., Hu, X., Lin, M., Zhang, Y., and Chen, Y. (2011). Functional redundancy between human SHOX and mouse Shox2 genes in the regulation of sinoatrial node formation and pacemaking function. J. Biol. Chem. *286*, 17029–17038.
41. Brown, L., Paraso, M., Arkell, R., and Brown, S. (2005). In vitro analysis of partial loss-of-function ZIC2 mutations in holoprosencephaly: Alanine tract expansion modulates DNA binding and transactivation. Hum. Mol. Genet. *14*, 411–420.
42. Bachetti, T., Matera, I., Borghini, S., Di Duca, M., Ravazzolo, R., and Ceccherini, I. (2005). Distinct pathogenetic mechanisms for PHOX2B associated polyalanine expansions and frameshift mutations in congenital central hypoventilation syndrome. Hum. Mol. Genet. *14*, 1815–1824.
43. Biressi, S., Messina, G., Collombat, P., Tagliafico, E., Monteverde, S., Benedetti, L., Cusella De Angelis, M.G., Mansouri, A., Ferrari, S., Tajbakhsh, S., et al. (2008). The homeobox gene Arx is a novel positive regulator of embryonic myogenesis. Cell Death Differ. *15*, 94–104.
44. Takeuchi, T., Yamazaki, Y., Katoh-Fukui, Y., Tsuchiya, R., Kondo, S., Motoyama, J., and Higashinakagawa, T. (1995). Gene trap capture of a novel mouse gene, jumonji, required for neural tube formation. Genes Dev. *9*, 1211–1222.
45. Miura, H., Yanazawa, M., Kato, K., and Kitamura, K. (1997). Expression of a novel aristaless related homeobox gene 'Arx' in the vertebrate telencephalon, diencephalon and floor plate. Mech. Dev. *65*, 99–109.
46. Friocourt, G., Kanatani, S., Tabata, H., Yozu, M., Takahashi, T., Antypa, M., Raguénès, O., Chelly, J., Férec, C., Nakajima, K., and Parnavelas, J.G. (2008). Cell-autonomous roles of ARX in cell proliferation and neuronal migration during corticogenesis. J. Neurosci. *28*, 5794–5805.
47. Xu, J., Deng, X., and Disteche, C.M. (2008). Sex-specific expression of the X-linked histone demethylase gene Jarid1c in brain. PLoS ONE *3*, e2553.
48. Colasante, G., Sessa, A., Crispi, S., Calogero, R., Mansouri, A., Collombat, P., and Broccoli, V. (2009). Arx acts as a regional key selector gene in the ventral telencephalon mainly through its transcriptional repression activity. Dev. Biol. *334*, 59–71.
49. Tahiliani, M., Mei, P., Fang, R., Leonor, T., Rutenberg, M., Shimizu, F., Li, J., Rao, A., and Shi, Y. (2007). The histone H3K4 demethylase SMCX links REST target genes to X-linked mental retardation. Nature *447*, 601–605.
50. Fico, A., Manganelli, G., Simeone, M., Guido, S., Minchiotti, G., and Filosa, S. (2008). High-throughput screening-compatible single-step protocol to differentiate embryonic stem cells in neurons. Stem Cells Dev. *17*, 573–584.
51. Collombat, P., Mansouri, A., Hecksher-Sorensen, J., Serup, P., Krull, J., Gradwohl, G., and Gruss, P. (2003). Opposing actions of Arx and Pax4 in endocrine pancreas development. Genes Dev. *17*, 2591–2603.
52. Galli, R., Fiocco, R., De Filippis, L., Muzio, L., Gritti, A., Mercurio, S., Broccoli, V., Pellegrini, M., Mallamaci, A., and Vescovi, A.L. (2002). Emx2 regulates the proliferation of stem cells of the adult mammalian central nervous system. Development *129*, 1633–1644.
53. Paciolla, M., Boni, R., Fusco, F., Pescatore, A., Poeta, L., Ursini, M.V., Lioi, M.B., and Miano, M.G. (2011). Nuclear factor-kappa-B-inhibitor alpha (NFKBIA) is a developmental marker of NF-κB/p65 activation during in vitro oocyte maturation and early embryogenesis. Hum. Reprod. *26*, 1191–1201.
54. Fusco, F., Mercadante, V., Miano, M.G., and Ursini, M.V. (2006). Multiple regulatory regions and tissue-specific transcription initiation mediate the expression of NEMO/IKK-gamma gene. Gene *383*, 99–107.

55. Abrajano, J.J., Qureshi, I.A., Gokhan, S., Zheng, D., Bergman, A., and Mehler, M.F. (2009). REST and CoREST modulate neuronal subtype specification, maturation and maintenance. PLoS ONE *4*, e7936.
56. Olivetti, P.R., and Noebels, J.L. (2012). Interneuron, interrupted: Molecular pathogenesis of ARX mutations and X-linked infantile spasms. Curr. Opin. Neurobiol. *22*, 859–865.
57. Beguin, S., Crépel, V., Aniksztejn, L., Becq, H., Pelosi, B., Pallesi-Pocachard, E., Bouamrane, L., Pasqualetti, M., Kitamura, K., Cardoso, C., and Represa, A. (2012). An Epilepsy-Related ARX Polyalanine Expansion Modifies Glutamatergic Neurons Excitability and Morphology Without Affecting GABAergic Neurons Development. Cereb. Cortex. Published online May 24, 2012.